J|A|C|S
ARTICLES
Published on Web 01/17/2007

Structural Assessment and Catalytic Consequences of the Oxygen Coordination Environment in Grafted Ti−Calixarenes

Justin M. Notestein,[†] Leandro R. Andrini,[‡] Vitaly I. Kalchenko,[§] Felix G. Requejo,*[,‡] Alexander Katz,*[,†] and Enrique Iglesia*[,†]

Contribution from the Department of Chemical Engineering, University of California at Berkeley, Berkeley, California 94720, Departamento de Física, Facultad de Ciencias Exactas, Universidad Nacional de La Plata and IFLP-INIFTA (CONICET), 1900 La Plata, Argentina, Institute of Organic Chemistry, National Academy of Sciences of Ukraine, Murmanskaya Str., 5, 02094, Kyiv-94, Ukraine

Received August 10, 2006; E-mail: requejo@fisica.unlp.edu.ar; askatz@berkeley.edu; iglesia@cchem.berkeley.edu

Abstract: Calixarene−Ti complexes were grafted onto SiO_2 (0.18−0.24 Ti nm^{-2}) to form isolated and accessible Ti centers persistently coordinated to multidentate calixarene ligands. Grafted Ti−*tert*-butylcalix[4]arenes gave Ti K-edge absorption spectra with pre-edge features at 4968.6−4968.9 eV, independently of Ti surface density and of their use in epoxidation catalysis. The structure and reactivity of grafted Ti−calix[4]arenes were weakly dependent on thermal treatment below 573 K, and the relative epoxidation rates of *trans*- and *cis*-alkenes showed that calixarene ligands did not restrict access to Ti centers more than corresponding calcined Ti−SiO_2 materials. For all materials, ^{13}C NMR and UV−visible spectroscopies confirmed the presence of Ti−O−Si connectivity and identical ligand-to-metal transitions. Grafted Ti−homooxacalix[3]arene complexes, however, gave weaker pre-edge features at higher energies (~4969.5 eV), consistent with greater Ti 3d occupancy and coordination numbers greater than four, and 20-fold lower cyclohexene epoxidation rate constants (per Ti) than on calix[4]arene-based materials. These different rates and near-edge spectra result from aldehyde formation caused by unimolecular cleavage of ether linkages in homooxacalix[3]arene ligands during grafting, leading to higher coordination and electron density at Ti centers. Materials based on *tert*-butylcalix[4]arene and homooxacalix[3]arenes led to similar epoxidation rates and near-edge spectra after calcination, consistent with the conversion of both materials to isolated Ti centers with identical structure. These materials provide a systematic approach for relating oxidation reactivity to Ti 3d occupancy, a descriptor of Lewis acid strength, and Ti coordination, because they provide Ti centers with varying electron density and coordination, but maintain accessible active centers with uniform structure and unrestricted access to reactants.

Introduction

Highly dispersed Ti centers dispersed onto or within SiO_2 frameworks are active catalysts for selective oxidations and other molecular rearrangements catalyzed by Lewis acids,[1−4] because the resulting 4-coordinate Ti centers are electron deficient and can expand their coordination to bind oxidants or substrates and to activate oxidants toward attack by electron-rich substrates. These Ti centers have been widely studied since the first reports of TS-1[5] and MCM41-grafted Cp_2TiCl_2[6] materials as prototypical Ti−SiO_2 catalysts. Previous studies have tried to develop routes for the synthesis of isolated Ti centers. UV−visible[7−9] and infrared and Raman[10−13] spectroscopies can probe various structural and electronic features of isolated Ti sites. Ti K-edge X-ray absorption spectroscopy remains, however, the method of choice to probe the local coordination of dispersed Ti structures.[10,14]

We report here the use of X-ray absorption methods on surface-grafted Ti−SiO_2 catalysts based on calixarene−Ti complexes **2a** and **2b** (Scheme 1), which catalyze epoxidation reactions with turnover rates independent of Ti surface density. Such properties are accepted hallmarks of uniform single-site catalysts[15] and evidence for isolated 4-coordinate Ti centers.

[†] University of California at Berkeley.
[‡] Universidad Nacional de La Plata and IFLP-INIFTA (CONICET).
[§] National Academy of Sciences of Ukraine.

(1) Sheldon, R. A.; van Doorn, J. A. *J. Catal.* **1973**, *31*, 427−437.
(2) Corma, A. *Catal. Rev. Sci. Eng.* **2004**, *46*, 369−417.
(3) Thomas, J. M.; Raja, R.; Lewis, D. W. *Angew. Chem., Int. Ed.* **2005**, *44*, 6456−6482.
(4) Davis, R. J.; Liu, Z. *Chem. Mater.* **1997**, *9*, 2311−2324.
(5) Bellussi, G.; Carati, A.; Clerici, M. G.; Maddinelli, G.; Millini, R. *J. Catal.* **1992**, *133*, 220−230.
(6) Maschmeyer, T.; Rey, F.; Sankar, G.; Thomas, J. M. *Nature* **1995**, *378*, 159−162.
(7) Soult, A. S.; Pooré, D. D.; Mayo, E. I.; Stiegman, A. E. *J. Phys. Chem. B* **2001**, *105*, 2687−2693.
(8) Geobaldo, F.; Bordiga, S.; Zecchina, A.; Giamello, E.; Leofanti, G.; Petrini, G. *Catal. Lett.* **1992**, *16*, 109−115.
(9) Marchese, L.; Maschmeyer, T.; Gianotti, E.; Coluccia, S.; Thomas, J. M. *J. Phys. Chem. B* **1997**, *101*, 8836−8838.
(10) Bordiga, S.; Coluccia, S.; Lamberti, C.; Marchese, L.; Zecchina, A.; Boscherini, F.; Buffa, F.; Genoni, F.; Leofanti, G.; Petrini, G.; Vlaic, G. *J. Phys. Chem.* **1994**, *98*, 4125−4132.
(11) Lin, W. Y.; Frei, H. *J. Am. Chem. Soc.* **2002**, *124*, 9292−9298.
(12) Li, C. *J. Catal.* **2003**, *216*, 203−212.
(13) Dartt, C. B.; Davis, M. E. *Appl. Catal., A* **1996**, *143*, 53−73.
(14) Thomas, J. M.; Sankar, G. *Acc. Chem. Res.* **2001**, *34*, 571−581.

10.1021/ja065830c CCC: $37.00

Scheme 1[a,b]

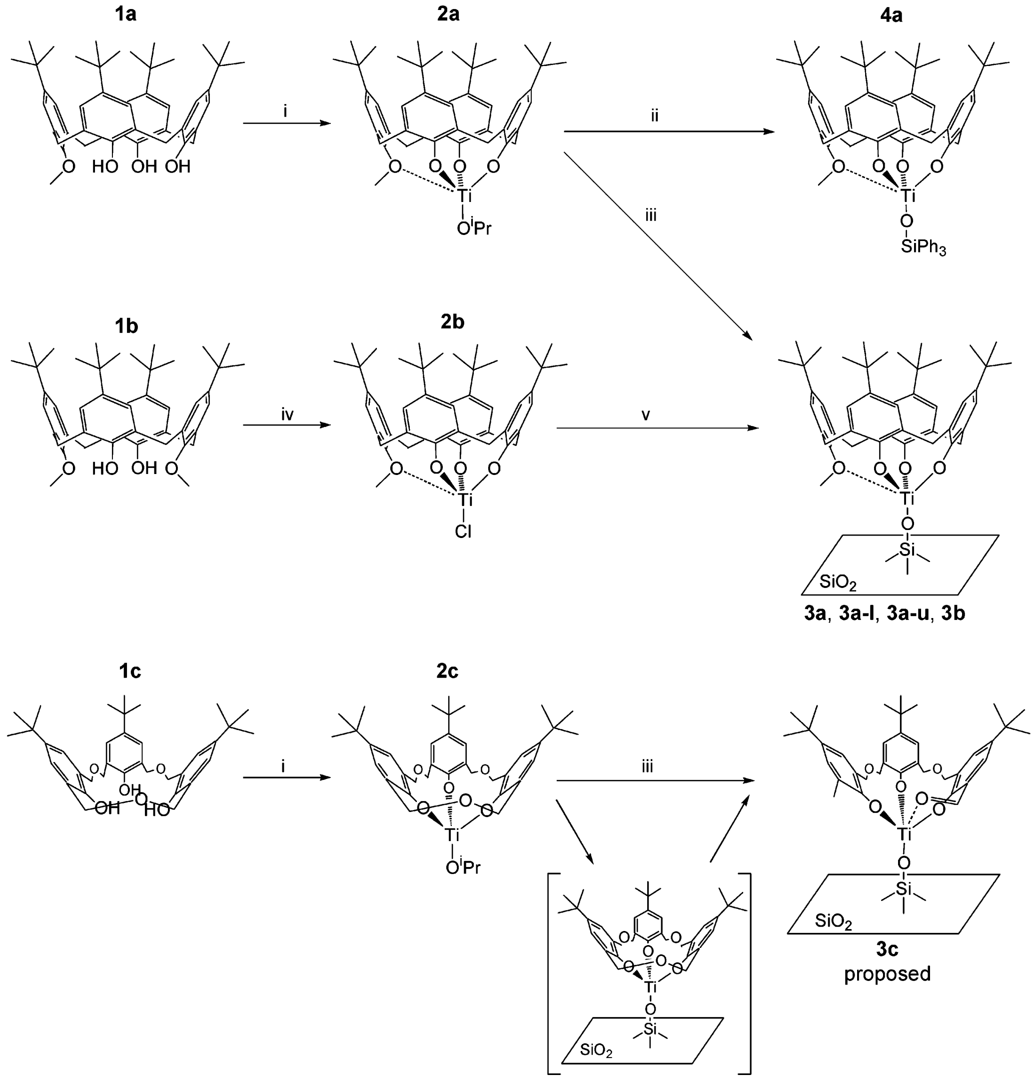

[a] Reactions and conditions: (i) Contact **1a** or **1c** with 1 equiv Ti(O^{i}Pr)$_4$ in toluene, 48 h; (ii) reflux **2a** with 1 equiv triphenylsilanol in toluene, 24 h; (iii) reflux **2a** or **2c** with partially dehydroxylated silica gel in toluene, 24 h; (iv) reflux **1b** with 1 equiv TiCl$_4$ in toluene, 24 h; (v) reflux **2b** with partially dehydroxylated silica gel and 10 equiv 2,6-di-*tert*-butylpyridine in toluene, 24 h. [b] Bracketed structure has not been isolated.

Single-site behavior, however, requires neither isolated Ti nor tetrahedral coordination; a notable example is the construction of identical 5-coordinate Ti−O−Ti dimers on SiO_2 under several grafting conditions.[16] Here, we use Ti K-edge X-ray absorption near-edge spectroscopy (XANES) to determine the Ti coordination number and the transition probability to unoccupied Ti 3d electronic states in these materials as a function of treatment temperature, Ti surface density, Ti precursor ($TiCl_4$ or TiO^{i}Pr$_4$), and catalyst use in epoxidation reactions. Calixarene−Ti and structurally related complexes have not been previously examined by XANES; in view of this, we prepared and characterized a soluble model compound **4a** as a standard material that contains all relevant calixarene−Ti and Ti−siloxy connectivities likely to exist in grafted complexes.

XANES is used here to measure the coordination number of surface-grafted Ti species coordinated to calixarene ligands, some of which may not persist during catalysis. We therefore turn to other calixarene macrocycles to demonstrate the relevance of these ligands to the Ti coordination in the resting state during catalytic turnovers. The substitution of some of the calixarene phenolic OH groups with methoxy groups can be used to vary the number of linkages between Ti centers and calixarene ligands,[17−22] but the catalytic consequences of these changes in coordination remain unexplored. Here, we show that grafting calix[4]arene−Ti complexes **2a** and **2b** leads to isolated 4-coordinate Ti, while homooxacalix[3]arene−Ti complexes **2c** (Scheme 1) also form isolated sites, but with Ti coordination greater than four. Grafting **2c** leads to lower epoxidation rates than calixarene complexes with 4-coordinate Ti centers, demonstrating the catalytic relevance of Ti−calixarene coordination and also that grafting of calixarene−Ti complexes leads to

(15) Notestein, J. M.; Iglesia, E.; Katz, A. *J. Am. Chem. Soc.* **2004**, *126*, 16478−16486.
(16) Bouh, A. O.; Rice, G. L.; Scott, S. L. *J. Am. Chem. Soc.* **1999**, *121*, 7201−7210.
(17) Dubberley, S. R.; Friedrich, A.; Willman, D. A.; Mountford, P.; Radius, U. *Chem. Eur. J.* **2003**, *9*, 3634−3654.
(18) Floriani, C.; Floriani-Moro, R. *Adv. Organomet. Chem.* **2001**, *47*, 167−233.
(19) Friedrich, A.; Radius, U. *Eur. J. Inorg. Chem.* **2004**, 4300−4316.
(20) Radius, U. *Inorg. Chem.* **2001**, *40*, 6637−6642.
(21) Zanotti-Gerosa, A.; Solari, E.; Giannini, L.; Floriani, C.; Re, N.; Chiesi-Villa, A.; Rizzoli, C. *Inorg. Chim. Acta* **1998**, *270*, 298−311.
(22) Radius, U.; Attner, J. *Eur. J. Inorg. Chem.* **1999**, 2221.

functional materials different from ligand-free Ti centers formed by oxidative treatments of organometallic precursors. The synthetic organic chemistry of macrocycles with varying coordination number and the subsequent grafting of their Ti complexes provide a route to develop new catalysts and to test the catalytic relevance of coordinative unsaturation in heterogeneous oxidation catalysis.

For Ti centers, an increase in the number of 3d electrons, determined by the number and identity of coordinating ligands, decreases Lewis acidity. In Ti K-edge XANES, the intensity of the pre-edge feature provides a direct measure of available Ti 3d orbitals.[23] The presence of intense XANES pre-edge features has been empirically related to the presence of 4-coordinate species and to highly active oxidation catalysts,[3,24−26] but a more complete analysis of the structural requirements for Ti-based Lewis-acid catalysis and of the fidelity of pre-edge features as descriptors of catalytic reactivity have remained elusive, at least in part because of the dearth of materials with uniform structure, accessible Ti centers, and coordination numbers larger than four. Sol−gel TiO_2-SiO_2 mixed oxides[27] and amorphous compounds containing Na_2O[28] have shown average Ti coordination numbers of five, but invariably contain a distribution of TiO_2 cluster sizes and Ti coordination numbers. In addition, the accessibility of Ti centers is incomplete and often uncertain. To our knowledge, JDF-L1[29] is the only synthetic material with only 5-coordinate Ti; it was reported to be active for phenol oxidation after HCl/H_2O_2 treatment, but rate data were not reported. Grafting 4-coordinate Ti centers on Sn- or Ge-modified SiO_2[30] alters the reactivity of Ti centers but without significant changes in near-edge spectra. The adsorption of amino alcohols or diamines onto preexisting Ti−SiO_2[31] markedly decreases epoxidation rates, but XANES data were not reported and the uniform nature of Ti centers remains unproven. The surface-grafted calixarene−Ti complexes reported here are ideally suited to probe the relation between near-edge features and turnover rates for various Ti environments, because of the common chemistries of the ligands involved and the uniform and accessible nature of the active Ti centers.

Experimental Methods

Ti K-XANES spectra were acquired using a fluorescence detector and a Si (111) monochromator at the D04B-XAS beamline of the LNLS (Laboratorio Nacional do Luz Síncrotron, Campinas, Brazil). Harmonic beam components were less than 1%, the incident beam energy was 1.37 MeV, and the resolution was 0.8 eV. The beam intensity was measured using ionization chambers filled with He at ambient temperature and pressure. Photon energies were calibrated in transmission mode by using a Ti foil placed between the second and third ionization chambers and setting the first inflection point at the known absorption edge energy of Ti^0 (4966 eV).[23] Energies below 4960 eV were fit to a Victoreen function and used to subtract background contributions throughout the entire energy range. Absorption intensities were normalized by their average value between 5050 and 5200 eV.[32]

Samples were treated at the specified temperature to remove adsorbed water and sealed into the sample holder within a controlled atmosphere box filled with dry Ar before measuring spectra. Untreated and liquid samples were sealed into the sample holder in ambient air. Spectra for soluble model compounds were measured using 0.1 M solutions in anhydrous toluene. Previous experimental and theoretical studies have identified three features in the Ti K-pre-edge region for anatase and other Ti oxides,[33−36] but higher energy resolution spectra have shown instead four distinct pre-edge features.[37−39] After background subtraction and normalization, the pre-edge region was fitted to four Gaussian peaks, labeled in ascending energy *A*1, *A*2, *A*3, and *B*, as in previous studies,[36,40] using WinXAS.[41]

Catalyst and model compound syntheses are illustrated in Scheme 1. All syntheses were performed using standard Schlenk line methods. Toluene was distilled in the presence of CaH_2 before use. Compound **1a** was synthesized from *tert*-butylcalix[4]arene (Aldrich, 95%) using accepted methods.[42] Compound **1b** was purchased from commercial sources (Acros, 99%). Compound **1c** was synthesized through an acid-catalyzed route.[43] Compounds **2a**[19] and **2c**[44] were synthesized by adding 1 equiv $Ti(O^iPr)_4$ (Aldrich 99.999%) to a 0.1 M toluene solution of **1a** or **1c** and stirring for 48 h. These reactions are known to proceed with nearly quantitative yields. Proton NMR resonances and mass spectrometry of these samples are consistent with published values. Compound **4a** was synthesized by adding a solution of **2a** to 1 equiv triphenylsilanol (Aldrich 98%) and refluxing for 24 h under flowing N_2. Its structure was verified by ^1H, ^{13}C, and ^{29}Si NMR spectroscopies, elemental analysis, and mass spectrometry, as described in the Supplemental Information. Catalysts **3a**−**l**, **3a**, and **3c** were prepared by adding, respectively, 0.1 mmol **2a**, 0.25 mmol **2a**, or 0.25 mmol **2c** per gram of SiO_2 (0.6 nm pore diameter, 250−500 μm particle diameter, partially dehydroxylated under dynamic vacuum at 773 K for 24 h, Selecto) in sufficient toluene to suspend the solids with magnetic stirring. The suspension was refluxed for 24 h and sparged with N_2 at 388 K until dry. The solids were washed with boiling toluene until calixarene complexes were no longer detected in the eluted liquids, and then dried under dynamic vacuum for 4 h at ambient temperature and for 4 h at 393 K.

Catalysts were stored in ambient conditions until use. The numbers listed after the dash in notation used herein indicate the treatment temperature in Ar before measuring Ti K-edge XANES spectra or in dynamic vacuum before measuring epoxidation rates or solid-state NMR spectra. Calixarene ligands were completely removed via treatment in flowing N_2/O_2 at 823 K to produce calcined materials **3a**-823 and **3c**-

(23) George, S. D.; Brant, P.; Solomon, E. I. *J. Am. Chem. Soc.* **2005**, *127*, 667−674.
(24) Blanco-Brieva, G.; Capel-Sanchez, M. C.; Campos-Martin, J. M.; Fierro, J. L. G.; Lede, E. J.; Adrini, L.; Requejo, F. G. *Adv. Synth. Catal.* **2003**, *345*, 1314−1320.
(25) Blasco, T.; Camblor, M. A.; Corma, A.; Pariente, J. P. *J. Am. Chem. Soc.* **1993**, *115*, 11806−11813.
(26) Blasco, T.; Corma, A.; Navarro, M. T.; Pariente, J. P. *J. Catal.* **1995**, *156*, 65−74.
(27) Beck, C.; Mallat, T.; Burgi, T.; Baiker, A. *J. Catal.* **2001**, *204*, 428−439.
(28) Ponader, C. W.; Boek, H.; Dickinson, J. E. *J. Non-Cryst. Solids* **1996**, *201*, 81−94.
(29) Roberts, M. A.; Sankar, G.; Thomas, J. M.; Jones, R. H.; Du, H.; Chen, J.; Pang, W.; Xu, R. *Nature* **1996**, *381*, 401−404.
(30) Oldroyd, R. D.; Sankar, G.; Thomas, J. M.; Özkaya, D. *J. Phys. Chem. B* **1998**, *102*, 1849−1855.
(31) Fraile, J. M.; García, J. I.; Mayoral, J. A.; Salvatella, L.; Vispe, E.; Brown, D. R.; Fuller, G. *J. Phys. Chem. B* **2003**, *107*, 519−526.
(32) Teo, B. K. *EXAFS: Basic Principles and Data Analysis*; Springer: New York, 1986.
(33) Chen, L. X.; Rajh, T.; Wang, Z. Y.; Thurnauer, M. C. *J. Phys. Chem. B* **1997**, *101*, 10688−10697.
(34) Uozumi, T.; Okada, K.; Kotani, A.; Durmeyer, O.; Kappler, J. P.; Beaurepaire, E.; Parlebas, J. C. *Europhys. Lett.* **1992**, *18*, 85−90.
(35) Wu, Z. Y.; Ouvrard, G.; Gressier, P.; Natoli, C. R. *Phys. Rev. B* **1997**, *55*, 10382−10391.
(36) Ruiz-Lopez, M. F.; Munoz-Paez, A. *J. Phys. Condens. Matter* **1991**, *3*, 8981.
(37) Brydson, R.; Sauer, H.; Engel, W.; Thomas, J. M.; Zeitler, E.; Kosugi, N.; Kuroda, H. *J. Phys. Condens. Matter* **1989**, *1*, 797−812.
(38) Matsuo, S.; Sakaguchi, N.; Wakita, H. *Anal. Sci.* **2005**, *21*, 805−809.
(39) Luca, V.; Djajanti, S.; Howe, R. F. *J. Phys. Chem. B* **1998**, *102*, 10650−10657.
(40) Grunes, L. A. *Phys. Rev. B* **1983**, *27*, 2111−2131.
(41) Ressler, T. *J. Synchrotron Radiat.* **1998**, *5*, 118.
(42) Groenen, L. C.; Ruël, B. H. M.; Casnati, A.; Verboom, W.; Pochini, A.; Ungaro, R.; Reinhoudt, D. N. *Tetrahedron* **1991**, *47*, 8379−8384.
(43) Miah, M.; Romanov, N. N.; Cragg, P. J. *J. Org. Chem.* **2002**, *67*, 3124−3126.
(44) Hampton, P. D.; Daitch, C. E.; Alam, T. M.; Bencze, Z.; Rosay, M. *Inorg. Chem.* **1994**, *33*, 4750−4758.

823. These materials were treated at 393 K in Ar or dynamic vacuum immediately prior to XANES spectra acquisition or measuring epoxidation rates, respectively. Compound **2b** and catalyst **3b** were prepared as described previously.[15] This preparation method includes treatment under dynamic vacuum for 1 h at 523 K immediately after synthesis. The material was stored in ambient air.

Thermogravimetric measurements were conducted (TGA 2950) in flowing dry N_2 or synthetic air (1.5 $cm^3\ s^{-1}$ N_2 or 0.5 $cm^3\ s^{-1}$ O_2 + 1.5 $cm^3\ s^{-1}$ N_2 as boil-off from liquid) by heating samples from ambient temperature to 1073 K at 0.083 K s^{-1} in a Pt pan. These methods were used to measure the number of calixarenes in each sample by assuming that the mass is lost by combustion of all organic fragments in calixarenes–Ti complexes **2a**, **2b**, or **2c**, with molecular weights of 654, 611, or 568, respectively. The presence of isopropoxide groups chemisorbed on the surface SiOH groups for **3a** and **3c** was confirmed by ^{13}C CP/MAS NMR and included in the calculation. This method predicts carbon contents in agreement with the 48:1, 45:1, and 39:1 C:Ti atom ratios expected from complexes **2a**, **2b**, and **2c**, respectively. Ti contents measured by Quantitative Technologies, Inc. using inductively coupled plasma mass spectrometry were 0.83, 0.48, and 0.67 wt % Ti for materials **3a**, **3a–l** and **3c**, respectively, and agree to within 5% of the surface densities calculated by TGA.

UV–visible spectra were measured at ambient conditions and temperature using a Varian Cary 400 Bio UV–visible spectrophotometer with a Harrick Praying Mantis accessory for diffuse-reflectance measurements of powders. Compressed poly(tetrafluoroethylene) was used as a perfect reflector standard to subtract background spectra and calculate pseudo-absorbances using the Kubelka–Munk formalism.[45] Solid-state ^1H MAS and ^{13}C CP/MAS NMR spectra were collected at the California Institute of Technology solid-state NMR facility using a Bruker DSX500 spectrometer operating at 500 MHz. Infrared spectra were measured using a Nicolet NEXUS 670 infrared spectrometer equipped with a Hg–Cd–Te (MCT) detector by averaging 5000 scans using samples diluted with KBr and held within a quartz vacuum cell with NaCl windows. Spectra were measured with 2 cm^{-1} resolution in the 4000 cm^{-1} – 400 cm^{-1} frequency region. Samples were heated in vacuum (<0.1 Torr) to 393 K (0.05 K s^{-1}) for 1 h before acquiring infrared spectra.

Cyclohexene epoxidation rates and selectivities were measured as follows: 30 mg catalyst and ~200 mg of zeolite A (previously dried at 573 K for 12 h in dynamic vacuum) were added to a 25 mL round-bottom flask and heated to the prescribed treatment temperature for 1 h in dynamic vacuum. The flask was filled under Ar and 20 mL anhydrous *n*-octane (Aldrich, 99.8%, passed over a SiO_2/Al_2O_3 column, and freshly distilled off Na metal) and 0.3 mL cyclohexene (Aldrich, 99%, passed over Al_2O_3 column, freshly distilled off CaH_2) were added to the reactor. The reactor was sealed and brought to 333 K. A solution of *tert*-butyl hydroperoxide (TBHP) in nonane (0.125 mL, 4.8 M solution in nonane, Aldrich, dried over 4A sieves) was added to initiate the reaction. Reaction rates and selectivities were measured by removing liquid aliquots and introducing them into a gas chromatograph (Agilent 6890, HP-1 methylsilicone capillary column).

Calixarene–Ti materials are highly selective, heterogeneous catalysts for epoxide synthesis and epoxidation rates obey the following rate equation at these reactant and catalyst concentrations:[15]

$$\text{rate} = \frac{d[\text{epoxide}]}{dt} = k_1[\text{Ti}][\text{alkene}][\text{TBHP}] \qquad (1)$$

where [Ti] is the total concentration of Ti centers in the reactor. All concentrations are in moles per L, resulting in a k_1 with units of $M^{-2}\ s^{-1}$. This rate constant (k_1, per Ti) was independent of Ti surface density, consistent with the uniform structure and single-site character of Ti centers in these samples.[15]

Materials **3a–u** and **3c–u** were used in epoxidation reactions, as described above, except with 300 mg catalyst, 50 mL *n*-octane, 0.81 mL cyclohexene, and 0.36 mL TBHP, which gave ~11 turnovers at 100% conversion. After 1 h the catalysts were hot filtered, washed with hot octane, and dried at 393 K for 1 h in dynamic vacuum. XANES and ^{13}C CP/MAS NMR spectra were measured to detect any changes in Ti coordination environment after catalysis.

Results and Discussion

Physicochemical Comparison of Materials 3a, 3b, and 3c. Materials **3a**, **3b**, and **3c** were prepared with an excess of calixarene–Ti precursors in the contacting solution, but they contain similar calixarene–Ti surface densities (0.18–0.24 Ti nm^{-2}), which correspond to at most 30% of the density of SiOH groups on the SiO_2 used.[46] This value resembles that for the maximum achievable density for random irreversible deposition[47] of non-interacting calixarenes ~1.5 nm in diameter. As shown for other calixarene–Ti materials,[15] this saturation behavior indicates that the Ti content is limited by the cross-sectional area of the calixarene ligand, whose steric bulk and tripodal chelation prevents Ti–O–Ti connectivity.

The proposed structures of these materials were confirmed by solid-state NMR and diffuse reflectance UV–visible spectroscopy. ^{13}C CP/MAS NMR spectra of **3a** and **3c** (Figure 1) give resonances at 67 and 22 ppm, indicative of isopropoxides adsorbed on silica (Si–O^{i}Pr),[16,48] without the sharp features at ~78 ppm[16] expected if Ti– O^{i}Pr connectivity persisted after grafting of Ti isopropoxide precursors. The other resonances for **3a** are similar to those for **2a** in solution[19] and to those for **3b**.[15] The solid-state NMR spectrum of **3a** is not visibly influenced, in chemical shift or intensity, by thermal treatment (up to 573 K) or by the use of the material in cyclohexene epoxidation.[15] The ^{13}C CP/MAS NMR spectrum of **3c** shows the aryl and *tert*-butyl resonances also present in the solution spectrum of **2c**,[44] together with weak resonances for benzyl ether bridging groups (resonance 4). The spectrum for **3c** also shows a new resonance at ~190 ppm, which suggests the presence of carbonyl groups (resonance 8). This conclusion is confirmed by the appearance of bands in the carbonyl region of the infrared spectra at 1560, 1640, and 1680 cm^{-1} (Figure S1) for this sample, which are absent for **1c**. These carbonyl signatures appear to reflect thermal and acid-catalyzed rearrangements of benzyl ether bridges[49] in the homooxacalix[3]arene ligand **1c** during grafting and thermal treatment to form an aldehyde and a methyl group. Grafted calix[4]arene material **3a** contains no features in the range of 1500–2000 cm^{-1}. Evidence of an aldehyde was obtained by extracting calixarene active sites from **3c** into $CDCl_3$ via treatment with trimethylsilyl chloride and subsequently observing a discrete resonance at 9.9 ppm in the solution ^1H NMR spectrum of the extracted sites.[50] The resulting carbonyl is likely to coordinate to the neighboring Ti center; indeed, salicylaldehyde–Ti complexes with simultaneous coordination of phenolate and aldehyde groups to a single Ti atom

(45) Delgass, W. N.; Haller, G. L.; Kellerman, R.; Lunsford, J. H. *Spectroscopy in Heterogeneous Catalysis*; Academic Press: New York, 1979.

(46) Zhuravlev, L. T. *Colloids Surf. A* **2000**, *173*, 1–38.

(47) Fadeev, A. Y.; Lisichkin, G. V. *Stud. Surf. Sci. Catal.* **1996**, *99*, 191–212.

(48) Liepins, E.; Zicmane, I.; Lukevics, E. *J. Organomet. Chem.* **1986**, *306*, 167–182.

(49) Zinke, A.; Ziegler, E. *Ber. Deutsch. Chem. Ges.* **1941**, *11*, 1729–1805.

(50) **3c** (56 mg of material) (0.18 mmol Ti g^{-1}) was treated at 393 K under <50 mTorr vacuum for 30 min. Then 0.01 mmol trimethylsilyl chloride (20 equiv per Ti) in 1 mL of dichloromethane was added at room temperature, and the solution was stirred for 30 min, decanted, and filtered under inert atmosphere. The filtrate was concentrated under vacuum and analyzed via ^1H NMR spectroscopy in $CDCl_3$.

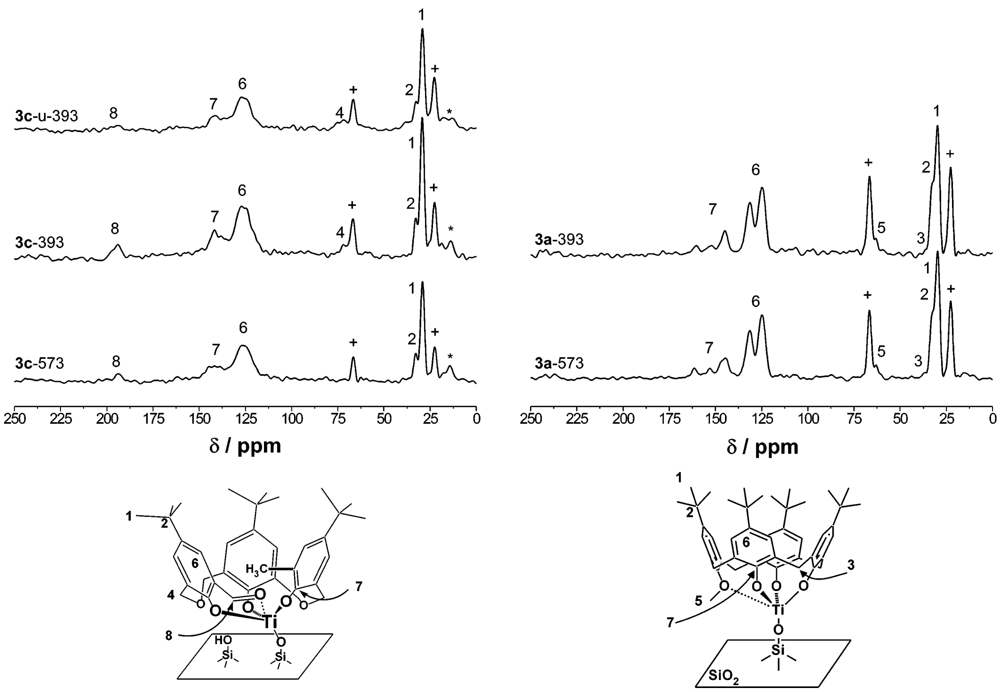

Figure 1. Solid-state ^{13}C CP/MAS NMR spectra of **3a** and **3c**. Resonances are labeled as in the accompanying structures. (*) indicates spinning sideband and (+) indicates resonances due to surface isopropoxy groups, the latter of which is emblematic of covalent surface grafting of the Ti complex. The resonance at ~190 ppm is indicative of a carbonyl group, whose intensity is extremely sensitive to catalyst pretreatment, presumably due to the long relaxation time of this group.

are known[51] and give carbonyl bands at ~1600 cm^{-1} shifted to lower frequencies from those in free salicyaldehyde ligand.[52] For **3c**, the carbonyl features in the NMR decreased in intensity, while the infrared band at 1640 cm^{-1} increased in intensity, after exposure to *tert*-butyl hydroperoxide, suggesting conversion of one carbonyl to another. Sequential aldehyde oxidation to an arenecarboxylic acid under reaction conditions cannot be ruled out.[53,54]

The calixarene−Ti ligand-to-metal charge transfer (LMCT) band responsible for the absorption edge[55,56] in UV−visible spectra (Figure S2) confirmed the calixarene−Ti connectivity shown in Scheme 1. The edge energies occur at 2.20 and 2.22 ± 0.04 eV for **3a** and **3c**, respectively. A similar edge energy (2.18 eV) was previously observed for **3b**,[15] indicating that the proposed Ti−phenolate connectivity is present and similar in these three samples. Soluble compound **4a** (0.1 mM in chloroform) gives an edge energy of 2.37 eV; a small red shift in the LMCT band is expected[57] as the species move from the low dielectric chloroform solution to a hydroxylated SiO_2 surface with a higher dielectric constant.[58] Comparisons between solution and solid-state NMR and the insensitivity of the LMCT energy to Ti surface coverage were previously used to show that **3b** consists of uniform Ti centers on a SiO_2 surface.[15] The similarity of the physicochemical characterization data for **3a** and **3c** to those for **3b** suggests that the former also consist of a single type of catalytic site, and that, with the exception of the presence of isopropoxide groups co-grafted on SiO_2, **3a** is indistinguishable from **3b**.

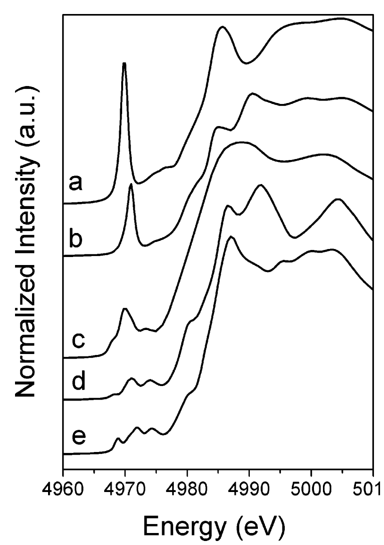

Figure 2. Ti K-XANES spectra of reference Ti-compounds at ambient temperature in air: (a) 4-fold coordinate $^{[4]}$Ti in Ba_2TiO_4; (b) $^{[5]}$Ti in Fresnoite; (c) $^{[5]}$Ti in nanostructured anatase (average crystal size <6 nm),[59] (d) $^{[6]}$Ti in rutile, and (e) $^{[6]}$Ti in anatase.

Coordination Environment of Calix[4]**arene Complexes.** Figure 2 shows Ti K-edge XANES spectra for Ti oxides and Ti silicates with known structures. Near-edge spectra for all samples showed a predominant pre-edge feature at ~4969 eV (Figure 3), as in 4-coordinate Ti ($^{[4]}$Ti) in Ba_2TiO_2 and 5-coordinate Ti ($^{[5]}$Ti) in the mineral fresnoite. Ti K-edge XANES spectra for **3a** are also reported in Figure 3 as a function

(51) Pennington, D. A.; Clegg, W.; Coles, S. J.; Harrington, R. W.; Hursthouse, M. B.; Hughes, D. L.; Light, M. E.; Schormann, M.; Bochmann, M.; Lancaster, S. J. *Dalton Trans.* **2005**, 561−571.
(52) Chaudhry, S. C.; Bhatt, S. S.; Sharma, N. *Ind. J. Chem.* **1996**, *35A*, 520.
(53) Subrahmanyam, C.; Louis, B.; Viswanathan, B.; Renken, A.; Varadarajan, T. K. *Appl. Catal., A* **2005**, *282*, 67−71.
(54) Wojtowicz, H.; Brzaszcz, M.; Kloc, K.; Mlochowski, J. *Tetrahedron* **2001**, *57*, 9743−9748.
(55) Barton, D. G.; Shtein, M.; Wilson, R. D.; Soled, S. L.; Iglesia, E. *J. Phys. Chem. B* **1999**, *103*, 630−640.
(56) Gao, X.; Bare, S. R.; Fierro, J. L. G.; Banares, M. A.; Wachs, I. E. *J. Phys. Chem. B* **1998**, *102*, 5653−5666.
(57) Lever, A. B. P. *Inorganic Electronic Spectroscopy*; Elsevier: New York, 1984.
(58) Bass, J. D.; Solovyov, A.; Pascall, A. J.; Katz, A. *J. Am. Chem. Soc.* **2006**, *128*, 3737−3747.

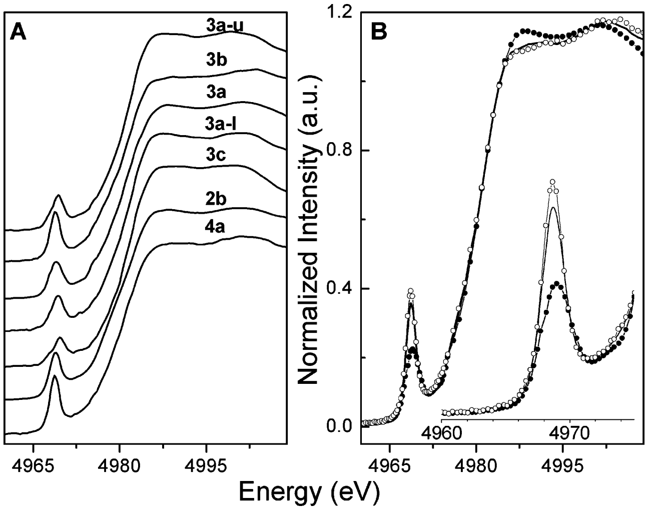

Figure 3. Ti K-edge XANES spectra of (A) all analyzed samples as synthesized and (B) details of XANES spectra evolution on **3a** as prepared, in air (−●−); in an Ar atmosphere after dehydration in Ar, 2 h at 393 K (−); and in an Ar atmosphere after dehydration in Ar, 2 h at 523 K (−○−). The inset amplifies the corresponding pre-edge region.

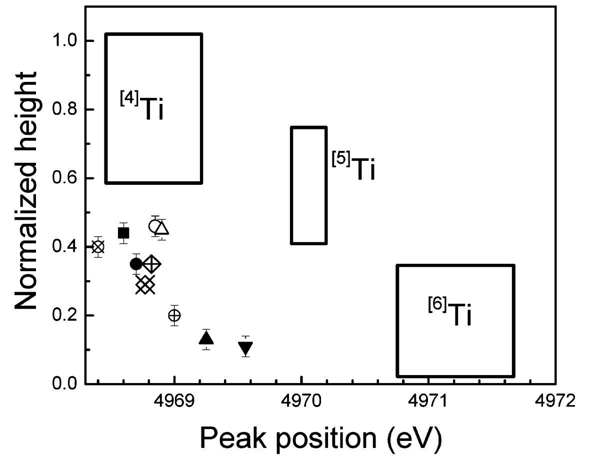

Figure 4. Position and intensity of the maximum of the pre-edge region of the XANES spectra for Ti-containing materials and compounds. Compounds **2b** (+) and **4a** (×) were analyzed in toluene solution. Powder materials and pretreatment temperatures in K are as follows: **3a**-none (⊕), **3a**-393 (●), **3a**-523 (⊗), **3a**-823 (○), **3b**-393 (■) **3c**-none (▼), **3c**-393 (▲), and **3c**-823 (△). Data for **3a−l** and **3a−u** are close to those of **4a** and are not plotted here for clarity. Rectangles show the region for each Ti coordination in Ti oxides and silicates, as taken from Farges et al.[61]

of treatment temperature; they are typical of those for all materials based on calix[4]arene−Ti complexes **2a** and **2b**. As shown previously for dispersed surface[56] and bulk framework[10,25,26] Ti centers in SiO_2 structures, pre-edge intensities for **3a** increased after treatment at 393 K in Ar, because the Ti coordination number decreases upon removal of water adsorbed during exposure to ambient air. Higher treatment temperatures (up to 523 K) did not cause any additional changes in pre-edge intensity, indicating that, as in the case of TS-1,[10] materials based on **2a** and **2b** are essentially free of adsorbed water at 393 K. Thermal treatments (up to 523 K) did not increase the X-ray absorption pre-edge intensity of **3c**, suggesting that its Ti centers are unaffected by atmospheric moisture and resistant to changes in ligand structure in this temperature range.

Phenomenological relations between the coordination symmetry of Ti atoms in Ti oxides[60] and silicates[61] and the position and intensity of the pre-edge feature in Ti K-edge spectra have been reported. Energies and intensities characteristic of 4-, 5-, and 6-fold coordination are shown in Figure 4 for natural minerals and for the catalysts and compounds used here. These data show that catalysts and compounds based on calix[4]arene−Ti complexes **2a** and **2b** give peak energies characteristic of $^{[4]}$Ti (4968.6 eV - 4968.8 eV), but relative peak heights more typical of $^{[5]}$Ti or $^{[6]}$Ti (0.2−0.5). If these materials contained pure Ti oxides or silicates, these energies and intensities could be interpreted as evidence for a mixture of $^{[4]}$Ti and $^{[6]}$Ti centers.[60,61] Lower intensities and energies than expected for $^{[4]}$Ti, however, can also reflect a higher occupancy of 3d states than for $^{[4]}$Ti sites within Ti oxides[60] or silicates as a result of non-oxide ligands and of the resulting distortion from tetrahedral symmetry. Such distortions prevail in other catalytically relevant Ti−SiO_2 materials and are expected also for materials based on **2a**.

Anhydrous TS-1 with tetrahedral symmetry (pre-edge height = 0.85)[10,62] and homogeneous $Ti(OSiPh_3)_4$ (pre-edge height = 0.80)[63] exhibit intense pre-edge features similar to those in $^{[4]}$Ti centers within natural minerals. Surface-grafted $^{[4]}$Ti in anhydrous Ti↑MCM41 (height = 0.55)[6] and Ti−silsesquioxane monomers (height = 0.60)[63], however, are distorted from tetrahedral symmetry by the $Ti(OSi)_3Y$ ligand field, in spite of their 4-fold coordination. Similarly, $Cp_xTiCl_{(4-x)}$ ($x = 0-2$) compounds exhibit similar near-tetrahedral symmetry for all values of x, but their pre-edge intensities differ because of the varying covalent character of their Ti−Cl bonds.[23] All these compounds have pre-edge intensities significantly lower than those for the $^{[4]}$Ti region shown in Figure 4.

Although Ti↑MCM41 and Cp_2TiCl_2 provide precedents for isolated $^{[4]}$Ti with pre-edge intensities lower than expected from tetrahedral coordination, we use soluble compounds **2b** and **4a** as model compounds to assign an unequivocal Ti coordination number to the grafted calixarene−Ti active sites in materials **3a** and **3b**. To assign the coordination number to the experimentally observed XANES spectra of compounds **2b** and **4a**, we use the previously determined single-crystal X-ray diffraction structure of **2b**[21] and, because **4a** has not been successfully crystallized, the structure of a V^{4+} analogue[64] of **4a**. Metal centers in **2b** and **4a** are connected to three calixarene phenols at ∼0.18 nm, in a geometry also found in other calixarene−Ti complexes.[17,19,20,22,65] The remaining phenolic O-atom lies 0.23−0.24 nm from the Ti atom, significantly farther than oxygen atoms in the first coordination sphere of fresnoite[66] or anatase,[67] and even farther than in H_2O physisorbed on TiO_2(110),[68] which occurs at 0.22 nm and is not generally observed to influence

(59) Stewart, S. J.; Fernandez-Garcia, M.; Belver, C.; Mun, S. B.; Requejo, F. G. *J. Phys. Chem. B* **2006**, *110*, 16482−16486.
(60) Waychunas, G. A. *Am. Mineral.* **1987**, *72*, 89−101.
(61) Farges, F.; Brown, G. E.; Rehr, J. J. *Phys. Rev. B* **1997**, *56*, 1809−1819.
(62) Davis, R. J.; Liu, Z.; Tabora, J. E.; Wieland, W. S. *Catal. Lett.* **1995**, *34*, 101.
(63) Thomas, J. M.; Sankar, G.; Klunduk, M. C.; Attfield, M. P.; Maschmeyer, T.; Johnson, B. F. G.; Bell, R. G. *J. Phys. Chem. B* **1999**, *103*, 8809−8813.
(64) Hoppe, E.; Limberg, C.; Ziemer, B.; Mugge, C. *J. Mol. Catal. A: Chem.* **2006**, *251*, 34−40.
(65) Olmstead, M. M.; Sigel, G.; Hope, H.; Xu, X.; Power, P. P. *J. Am. Chem. Soc.* **1985**, *107*, 8087−8091.
(66) Moore, P. B.; Louisnat, Sj. *Z. Kristallogr.* **1969**, *130*, 438−448.
(67) Horn, M.; Schwerdt, Cf.; Meagher, E. P. *Z. Kristallogr.* **1972**, *136*, 273−281.
(68) Allegretti, F.; O'Brien, S.; Polcik, M.; Sayago, D. I.; Woodruff, D. P. *Phys. Rev. Lett.* **2005**, *95*, 226104.

pre-edge spectral features. Although the interaction between the Ti atom and the ether oxygen is detected by shifts in the ^{13}C NMR spectrum,[15] it is expected to be very weak and not to lead to detectable features in the near-edge or fine structure of X-ray absorption spectra because of the Ti−O distance and the thermal and structural disorder expected in both supported and solution species. For compounds **4a** and **2b**, the Ph_3SiO^- or Cl^- ligands make up the fourth coordinating species; we therefore consider the experimental XANES pre-edge positions and intensities of these two soluble compounds (4968.8 eV and 0.29−0.35 relative intensity) to reflect the presence of isolated and nearly 4-coordinate calixarene−Ti.

The XANES pre-edge peak location and intensity for catalysts based on **2b** or **2c** and treated above 393 K lie within 0.1 eV and 0.1 intensity units of those for model compounds **2b** and **4a** in solution (Figure 4). Taken together with the finding that epoxidation turnover rates on **3b** are similar to those on other isolated Ti−SiO_2 catalysts,[15] these data indicate the prevalence of $^{[4]}$Ti in these materials. All catalysts based on calix[4]arene, irrespective of calixarene−Ti surface density, Ti precursor type (chloride or isopropoxide), or use in epoxidation catalysis give similar near-edge spectra, which resemble those for the soluble model compounds. These similarities strongly suggest that the SiO_2 surface acts as a monodentate ligand similar to Ph_3SiO^- in **4a**, and that the calixarene−Ti connectivity is retained in all these materials, consistent with their nature and function as single-site 4-coordinate Ti active centers.

Coordination Environment of Homooxacalix[3]arene Complexes. In contrast with the similar XANES spectra of all materials and compounds based on calixarene−Ti complexes **2a** and **2b**, pre-edge features for **3c** are much weaker (~0.1 vs ~0.35) and occur at higher energies (by >0.4 eV). This indicates a higher average Ti coordination number than in **3a** and **3b** and in compounds **2b** and **4a**. The spectrum for **3c** is unaffected by treatment temperatures up to 523 K; thus, the retention of ambient moisture is not responsible for its higher average Ti coordination. The energy of the pre-edge peak for **3c** lies between those for anatase and for samples with isolated $^{[4]}$Ti, as in small TiO_2 crystallites,[33,39,69,70] TiO_2 containing O vacancies[59,71] (Figure 2c), or nitrogen-doped TiO_2,[72] for which oxygen vacancies or the prevalence of surface Ti atoms leads to average Ti coordination numbers of ~5. These analogies lead us to propose that Ti atoms in **3c** are also, on average, 5-coordinate. We also show below that this 5-fold coordination in **3c** arises from a derivative of the multidentate calixarene **1c** on isolated Ti centers, and not from the formation of small TiO_2 clusters.

UV−visible spectra show that calixarene−Ti connectivity exists in **3c**, and solid-state ^{13}C CP/MAS NMR spectra indicate that isopropoxide groups present in the Ti precursors used are no longer connected to Ti, consistent with covalent grafting of Ti−calixarenes onto SiO_2. Material **3c** has a calixarene surface density similar to that of catalysts **3a** and **3b**, corresponding to saturation coverages for random calixarene deposition. After calcination, materials **3c**-823 and **3a**-823 give similar UV−visible spectra (Figure S2), which, as shown for other calcined Ti−SiO_2 materials,[8,10,73,74] suggests a similar Ti dispersion for these two samples. Most importantly, the relative pre-edge heights of the XANES spectra of **3a**-823 and **3c**-823 are identical within the accuracy of the measurements, confirming the similar dispersion in these two materials. Moreover, the relative pre-edge heights of these materials (0.46 for both) are comparable to other highly dispersed Ti−SiO_2 materials such as Ti↑MCM41 (height = 0.55)[6]. From these results, we conclude that Ti atoms in material **3c** are as isolated and uniformly dispersed as in materials **3b** and **3c**. This Ti site isolation and the differences in the XANES spectra for as-synthesed **3a** and **3c** are both a consequence of the persistent coordination of bulky multidentate ligands.

We have shown above that calix[4]arene−Ti complexes **2a** and **2b** create $^{[4]}$Ti atoms when grafted on SiO_2 surfaces. Calixarene **1c** contains only three phenolic oxygens; thus, any additional coordination to Ti in **3c** would require O-atoms from the macrocycle, from silica, or from any adsorbed water retained at 523 K. Compounds **2a** and **2c** were grafted onto identical supports; thus, we expect that SiO_2 acts as a monodentate ligand for **3c**, as it does for **3a**. Water can be stabilized by interactions with metal centers within cavities in calixarene−metal complexes,[22,75,76] but we find no evidence here for such host−guest complexes. Single-crystal X-ray diffraction structures for **2c**[77] do not show any Ti atoms within 0.24 nm of the ether oxygens; thus, such Ti−O interactions, if present, are not expected to influence the near-edge spectra, as discussed above. We find, however, carbonyl resonances in the solid-state ^{13}C CP/MAS NMR spectra of **3c** and vibrational bands in its infrared spectrum, suggesting that salicylaldehyde-type structures (Scheme 1) may be present. Persistent coordination of Ti to three phenols, the SiO_2 surface, and a carbonyl formed from the dibenzyl ethers in the **1c** macrocycle, as discussed in above, appears to account for the higher than 4-fold Ti coordination in **3c**. The spectroscopic resemblance of materials **3c** and **3a**, except for the additional carbonyl coordination to Ti centers, provides an excellent molecular system, with well-defined coordination and complete accessibility, to test the effects of Ti−O coordination on epoxidation turnover rates.

Calixarene−Ti Catalytic Reactivity. Materials based on **2b** are active and selective catalysts for epoxidation of alkenes by alkyl hydroperoxides.[15] Here, materials based on **2a** and **2c** were used for epoxidation of cyclohexene and 2,5-dimethyl-3-hexene using TBHP in *n*-octane at 333 K to probe the catalytic consequences of calixarene ligands and Ti coordination on epoxidation catalysis. Cyclohexene epoxidation on **3a** reached 50% conversion of TBHP in ~2 h, and continued to nearly complete TBHP conversions (>95%). More than 90% of the TBHP converted is used in epoxidation reactions and no oxidation products (e.g., cyclohexene-one, cyclohexene-ol, cyclohexane-diol, or C8 alcohols) except cyclohexene epoxide were detected, indicating that TBHP losses reflect only adsorption onto SiO_2 surfaces. Epoxide ring-opening was avoided by maintaining strictly anhydrous conditions,[78,79] and to a lesser

(69) Chen, L. X.; Rajh, T.; Jager, W.; Nedeljkovic, J.; Thurnauer, M. C. *J. Synchrotron Radiat.* **1999**, *6*, 445−447.
(70) Fernandez-Garcia, M.; Martinez-Arias, A.; Hanson, J. C.; Rodriguez, J. A. *Chem. Rev.* **2004**, *104*, 4063−4104.
(71) Belver, C.; Bellod, R.; Stewart, S. J.; Requejo, F. G.; Fernandez-Garcia, M. *Appl. Catal., B* **2006**, *65*, 309−314.
(72) Batzill, M.; Morales, E. H.; Diebold, U. *Phys. Rev. Lett.* **2006**, *96*, 026103.
(73) Hutter, R.; Mallat, T.; Baiker, A. *J. Catal.* **1995**, *153*, 177−189.
(74) Fraile, J. M.; Garcia, J. I.; Mayoral, J. A.; Vispe, E. *J. Catal.* **2005**, *233*, 90−99.
(75) Mongrain, P.; Douville, J.; Gagnon, J.; Drouin, M.; Decken, A.; Fortin, D.; Harvey, P. D. *Can. J. Chem.* **2004**, *82*, 1452−1461.
(76) Acho, J. A.; Doerrer, L. H.; Lippard, S. J. *Inorg. Chem.* **1995**, *34*, 2542−2556.
(77) Hampton, P. D.; Daitch, C. E.; Alam, T. M.; Pruss, E. A. *Inorg. Chem.* **1997**, *36*, 2879−2883.

Table 1. XANES Pre-edge Features and Epoxidation Rate Constants Per Ti for Experimental Materials

	calix–Ti nm^{-2}	pretreatment T (K)	pre-edge[a] position (eV)	height (I/I_0)	$(A_{A2} + A_{A3})/A_T$[b]	epoxidation rate[c] k_1 (M^{-2} s^{-1})
2b	n/a	n/a	4968.8	0.35	0.83	0.1[d]
4a	n/a	n/a	4968.8	0.29	0.77	0.4
3a	0.22	none[e]	4969.0	0.20	0.78	7.9
3a	0.22	393	4968.7	0.35	0.83	6.9
3a	0.22	523	4968.4	0.40	0.86	5.8
3a	0.22	573	–	–	–	5.7
3a	0.22	823[f]	4968.9	0.46	0.78	4.6
3a–u	0.22	393	4968.9	0.30	0.77	–
3a–l	0.13	393	4968.8	0.26	*g*	–
3b	0.24	393	4968.6	0.44	0.89	11.1[d]
3c	0.18	none[e]	4969.6	0.11	0.54	0.4
3c	0.18	393	4969.3	0.13	0.58	0.5
3c	0.18	523	*g*	0.11	*g*	0.7
3c	0.18	573	–	–	–	1.7
3c	0.18	823[f]	4968.9	0.45	0.71	3.6
anatase	n/a	none[e]				–

[a] ±0.1 eV, ±0.03 I/I_0. [b] Here, the area weighted average of the peak locations of features $A2$ and $A3$ agrees with the maximum of the total pre-edge feature. Relative areas are given as the area of peaks $A2 + A3$ versus the total area of all pre-edge peaks (A_T) ±0.07. [c] Epoxidation rate constant k_1 per Ti as described in Experimental Methods, M^{-2} s^{-1}. [d] From Notestein et al.[15] [e] XANES samples were measured as received, catalysis samples treated under dynamic vacuum 1 h at ambient temperature. [f] Calcined in flowing N_2/O_2. [g] Very low S/N, pre-edge feature cannot be accurately located or decomposed into individual Gaussians.

extent by the weak binding of ethers by Ti–calixarene complexes.[19,21] At the conditions used, contributions from radical oxidation processes are negligible.[15,80] Catalysts are compared here based on their rate constant k_1 (as given in eq 1; per Ti) for epoxide formation over the first 2 h of reaction (Table 1). As discussed previously, calix[4]arene-based catalysts such as **3b** are stable and do not leach active species or Ti, and their cyclohexene epoxidation rates are similar to those on other isolated Ti–SiO_2 materials when cumene hydroperoxide is used as the oxidant and at higher concentrations than used in this study.[15] The supernatant liquid phase in catalytic reaction mixtures of material **3c** is inactive for epoxidation, and the ^{13}C CP/MAS NMR and diffuse reflectance UV–visible spectra are not significantly changed in intensity after catalysis, proving the absence of leaching in these materials as well.

The relative epoxidation rates of *trans*- versus *cis*-2,5-dimethyl-3-hexene (normalized by their respective concentrations) were used to probe the relative accessibility of Ti centers in each catalyst. Alkene epoxidation rates are known to increase with increasingly electron-rich double bonds;[1] thus, *trans*/*cis* isomers are expected to have the same intrinsic reactivity, but any spatial constraints would restrict access preferentially for the bulkier *trans*-isomers. This rate ratio is ∼0.19 for both **3a**-393 and **3c**-393, indicating that Ti centers are similarly accessible in both catalysts.[81] Removal of the calixarene ligand to form **3a**-823 increases only slightly the trans/cis rate ratio (0.22); thus, calixarene ligands do not impede access to Ti centers grafted onto their lower rim. The stoichiometric oxidant *m*-chloroperbenzoic acid gives a rate ratio of 1.2 in noncatalytic epoxidation. Therefore, Ti centers grafted onto SiO_2 surfaces are spatially constrained relative to epoxidation of molecules in homogeneous media, but the severity of these constraints is affected only weakly by the additional presence and type of calixarene ligands. The pronounced sensitivity of these site-isolated grafted Ti catalysts to the steric bulk at the double bond requires that reaction of the alkene with the activated hydroperoxide occurs at or before the rate-limiting step in the epoxidation reaction.

In the absence of an organic ligand, the similar surface densities and accessibility of randomly distributed Ti centers in materials **3a** and **3c** suggest that these materials would show similar catalytic turnover rates. Instead, epoxidation rate constants per Ti for **3a** are up to 20 times greater than for **3c** after thermal treatments below 523 K (Table 1). Rate constants for **3a** decreased monotonically (by ∼30%) as the treatment temperature increased to 573 K. This decrease in reactivity occurred concurrently with a slight decrease in coordination number detectable in the near-edge spectrum (see Table 1); it may reflect the involvement of surface SiOH sites in kinetically relevant epoxidation elementary steps[27,82–86] and a concurrent decrease in their total number with increasing treatment temperature.[46] For **3c**, treatments below 523 K did not influence k_1, but higher temperatures (573–623 K) led to a sharp increase in epoxidation rate constants, concurrent with the decomposition of **3c**, detected by thermogravimetry (Figure S3). Complete oxidative removal of calixarene ligands for **3a-**823 and **3c-**823 led to a further decrease in k_1 for **3a** and an additional increase for **3c**. After this oxidative treatment, the catalytic rate constants (per Ti) of **3a**-823 and **3c**-823 differ by <25%, providing final evidence that Ti atoms in both materials are dispersed on the SiO_2 support to similar extents. That is, once the overriding influence of the organic calixarene ligand is removed, the catalytic reactivity and the XANES spectra discussed above are indicative of well-dispersed Ti centers on SiO_2, without any evidence for the formation of extended crystallites of TiO_2.

(78) Corma, A.; Domine, M.; Gaona, J. A.; Jordá, J. L.; Navarro, M. T.; Rey, F.; Pérez-Parienta, J.; Tsuji, J.; McCulloch, B.; Nemeth, L. T. *Chem. Commun.* **1998**, 2211–2212.
(79) Jarupatrakorn, J.; Tilley, T. D. *J. Am. Chem. Soc.* **2002**, *124*, 8380–8388.
(80) Oldroyd, R. D.; Thomas, J. M.; Maschmeyer, T.; MacFaul, P. A.; Snelgrove, D. W.; Ingold, K. U.; Wayner, D. D. M. *Angew. Chem., Int. Ed.* **1996**, *35*, 2787–2790.
(81) This test is insensitive to sites with spatial constraints so severe that sites become inactive.
(82) Wells, D. H.; Delgass, W. N.; Thomson, K. T. *J. Am. Chem. Soc.* **2004**, *126*, 2956–2962.
(83) Wells, D. H.; Joshi, A. M.; Delgass, W. N.; Thomson, K. T. *J. Phys. Chem. B* **2006**, *110*, 14627–14639.
(84) Urakawa, A.; Burgi, T.; Skrabal, P.; Bangerter, F.; Baiker, A. *J. Phys. Chem. B* **2005**, *109*, 2212–2221.
(85) Vayssilov, G. N.; van Santen, R. A. *J. Catal.* **1998**, *175*, 170–174.
(86) Beck, C.; Mallat, T.; Baiker, A. *New J. Chem.* **2003**, *27*, 1284–1289.

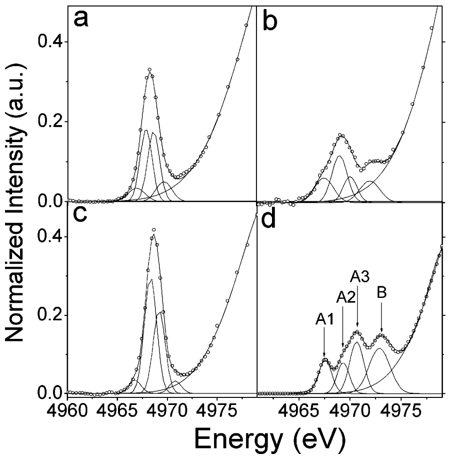

Figure 5. Representative fits of the pre-edge region of XANES spectra after treatment in Ar at 393 K for samples (a) **3a**−**u**, (b) **3c**, (c) **3b**, and (d) anatase ([6]Ti standard) measured at ambient temperature in air. For all spectra, the pre-edge region is resolved into four Gaussian peaks corresponding to different electronic transitions and labeled in order of ascending energy *A*1, *A*2, *A*3, and *B*.[40] An extra peak is fit to empirically account for edge rising. Fluorescence intensities are normalized by their average values between 5050 and 5200 eV.

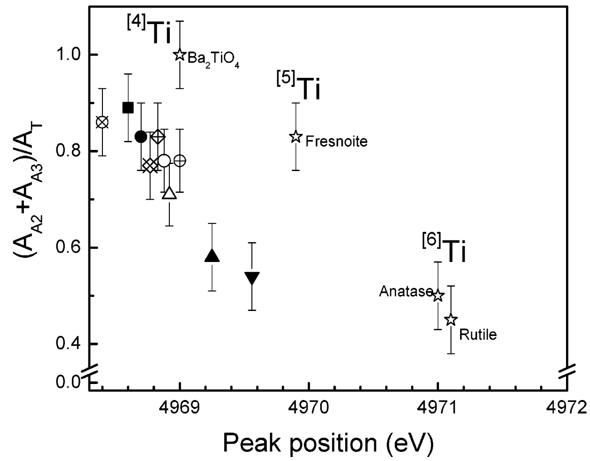

Figure 6. Position and relative area of peaks *A*2 and *A*3 for Ti-containing materials and compounds. Compounds **2b** (+) and **4a** (×) were analyzed in toluene solution. Powder materials and pretreatment temperatures in K are as follows: **3a**-none (⊕), **3a**-393 (●), **3a**-523 (⊗), **3a**-823 (○), **3b**-393 (■) **3c**-none (▼), **3c**-393 (▲), and **3c**-823 (△). Reference Ti oxides and silicates (*) are as indicated in the figure. Error bars are estimated from confidence of fitting procedures. The peak position of $A2 + A3$ is an area-weighted average and the sum of their areas are normalized with respect to the total pre-edge peak area ($A_T = A_{A1} + A_{A2} + A_{A3} + A_B$).

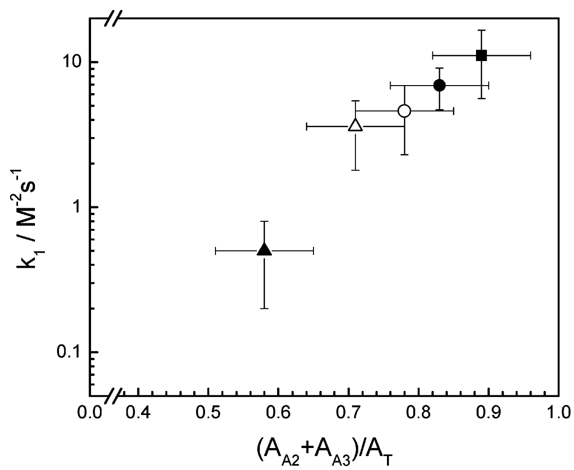

Figure 7. Epoxidation rate constants per Ti as a function of the relative area of peaks $A2 + A3$ for Ti-containing materials **3a**-393 (●), **3a**-823 (○), **3b**-393 (■), **3c**-393 (▲), and 3c-823 (△). Error bars are estimated from confidence of fitting procedures. Use of the $A2 + A3$ relative peak area rather than the total pre-edge feature height predicts a monotonic relationship between catalyst reactivity and Ti K-edge XANES for all calixarene-containing and calcined Ti−SiO_2 materials.

Comparison of Relative Pre-edge Areas and Epoxidation Rates. Materials based on **2a** and **2c** differ in epoxidation rates and in how ligand removal influences their reactivity. These materials were prepared by similar methods and exhibit identical UV−visible LMCT energies, steric constraints, and maximum Ti surface densities. After calixarene ligand removal, these materials exhibit similar turnover rates, XANES and UV-visible spectra. As a result, these materials provide excellent models for comparing the effects of Ti electron density, measured by XANES, on reactivity for molecular rearrangements catalyzed by Lewis acids.

Figure 4 shows average Ti coordination numbers in Ti oxides and silicates, as typically inferred from Ti K-edge XANES pre-edge peaks using methods first reported by Farges et al.[61] and Waychunas.[60] As in a recent study,[59] we deconvolute the relative intensities of the individual electronic transitions giving rise to the pre-edge features, as determined by Grunes,[40] as an improved method for assessing Ti coordination, especially for distorted environments prevalent specifically in 5-coordinated systems and more generally in highly dispersed materials. Specifically, we use the energy positions of transitions *A2* and *A3* (See Figure 5 for fits of representative materials) and their combined area relative to that of all pre-edge features as a measure of Ti 3d occupancy. As in the case of the overall pre-edge feature intensity and location, these relative peak areas can be related empirically to structures of known Ti coordination number, as in Figure 6. From this figure, it is immediately evident that materials **3a** and **3b** have approximately 4-coordinate structures, as predicted, and that the plot position of **3c** is consistent with 5-coordinate Ti centers. All compounds and catalysts derived from **2a** and **2b** show a higher relative intensity for peaks *A2* and *A3* than catalyst **3c**. Also, peaks $A2 + A3$ for catalysts based on **2a** and **2b** appear more than 0.4 eV below those for **3c**. These differences in peak position and intensity persist after all thermal treatments below 523 K (Table 1). This relative peak area provides a measure of the extent of Ti 3d orbital availability in these materials, an electronic feature of materials that is likely to correlate to binding and reactivity of molecules much more directly than a geometric description, such as coordination number.

We therefore use the relative $A2 + A3$ peak area as a continuous measure of Ti 3d occupancy and relate it here directly to epoxidation reactivity. Figure 7 shows cyclohexene epoxidation rate constants (k_1, per Ti, TBHP co-reactant) as a function of the relative intensity of peaks $A2 + A3$ for catalysts **3a**, **3b**, and **3c** pretreated at 393 K and after calcination. The almost linear correlation between relative peak intensities and the logarithm of k_1 suggests that epoxidation activation energies are indeed related to pre-edge features of Ti centers. This correlation persists over 20-fold changes in rates (∼8 kJ/mol in apparent activation energy). Moreover, even though materials **3a** and **3b** and both calcined materials would all be considered 4-coordinate, the overall correlation persists for small differences in rates and near-edge features. For example, the decrease in rate of **3a** after calcination is accompanied by a small decrease in the relative $A2 + A3$ area. Using the relative pre-edge feature height for the ordinate does not give such a monotonic correlation when calcined and calixarene-containing catalysts are compared together, indicating more general applicability when the relative $A2 + A3$ area is used. The similar linear-free energy relationship found for calixarene-containing and calcined materials indicates a similar epoxidation mechanism for both types of samples. A similar correlation between epoxidation yield with TBHP and XANES pre-edge features was developed for sol−gel TiO_2−SiO_2 materials,[87] further indicating the general nature of the trends shown in Figure 7.

In contrast to the trend identified above, compounds **2b** and **4a** give spectra nearly identical to those of **3a**, but their epoxidation rates are much smaller. The soluble catalysts must therefore be operating via a different mechanism than the heterogeneous catalysts or suffer from a rapid deactivation pathway (e.g., formation of unreactive dimer species) absent in immobilized materials of identical composition. These conclusions underscore the need to compare structurally and mechanistically similar catalysts, provided by the series of grafted calixarene−Ti materials described here, to reach relevant inferences and structure−function relations. The data in Figure 7 provide a rigorous correlation between d-orbital occupancy, Ti−O coordination, and epoxidation reactivity, which appears to be general for calixarene-containing and calcined materials, while also confirming that the structure of the grafted Ti−calixarene detected by X-ray absorption is preserved during catalytic epoxidation cycles. Furthermore, these data demonstrate that the presence of an additional donor ligand has a pronounced effect on epoxidation rates when comparing catalysts **3a** and **3c**. This is in contrast to predictions based on density functional theory that the epoxidation activation energy for oxygen transfer from TiOOR intermediates would be insensitive to the presence of an additional monodendate ligand.[88,89] Our results therefore suggest either a stronger metal−alkylhydroperoxide interaction than previously proposed or a strong decrease in the epoxidation pre-exponential factor when an additional coordinated ligand is part of a multidentate complex.

Conclusion

Titanium present in low concentrations in silicate frameworks as 4-coordinate species are known to be active for Lewis acid-catalyzed reactions, whereas 6-coordinate TiO_2 domains are generally inactive; less is known about intermediate geometries. The synthesis of new Ti−SiO_2 materials based on calixarene−Ti precursors provides access to 4-coordinate Ti using calix[4]arene−Ti complexes **2a** and **2b**, and higher coordination numbers using homoxacalix[3]arene−Ti **2c**. Diffuse reflectance UV−visible and solid-state NMR spectroscopy show that intact calixarene−Ti complexes are covalently grafted to the surface at densities corresponding to the maximum random packing of the calixarene ligand, ensuring site isolation of grafted Ti centers. Ti K-edge XANES spectra of all dried materials based on **2a** or **2b** indicate $^{[4]}$Ti with increased Ti 3d occupancy based on comparison to known Ti−SiO_2 catalysts and soluble calixarene−metal species with known single-crystal X-ray diffraction structures. In addition to the previously proven single-site catalytic behavior for these well-dispersed Ti-containing materials, these materials are also site-isolated Ti−SiO_2 catalysts. Moreover, the similarity of the XANES spectra regardless of calixarene−Ti surface density, use as an oxidation catalyst, or the identity of the non-calixarene ligand proves that the macrocyclic calixarene ligand acts as a template for the ultimate Ti coordination on the surface.

In contrast to the similar catalytic activity and structure of materials based on **2a** and **2b**, materials based on homoxacalix[3]arene−Ti **2c** possess an increased average Ti coordination number. This coordination number is persistent to 523 K, eliminating the possibility of simple coordination sphere expansion by a physisorbed species. The resulting catalyst **3c** also possesses a reactivity for epoxidation decreased by as much as 20 times in comparison to that of **3a**, indicating persistent coordination of the calixarene macrocycle during catalytic turnover. After ligand removal, **3c**-823 is similar to material **2a**-823 in both catalytic reactivity, UV−visible spectroscopy, and XANES, indicating that the degree of Ti isolation is similar in each case, and therefore that the differences in coordination number are solely due to the overriding influence of the different calixarene ligand geometries.

These calixarene−Ti−SiO_2 materials are used to develop a quantitative correlation between the occupancy of the Ti 3d orbital, as judged by the relative area of peaks $A2 + A3$ in the XANES pre-edge, and the rate constant for the epoxidation of cyclohexene using TBHP. A monotonic decrease in apparent activation energy over ~8 kJ/mol accompanies the increase in the relative $A2 + A3$ peak area for calixarene-containing and calcined catalysts. This result illustrates the utility of Ti XANES in quantitatively predicting Lewis-acid catalysis activity and proves that these calixarenes can be used to create new surface structures that are relevant during catalytic turnover and can be directly compared to solid oxide surfaces.

Acknowledgment. We acknowledge the financial support of the U.S. DOE Office of Basic Energy Sciences (DE-FG02-05ER15696). The technical assistance of Dr. Aditya Bhan with infrared measurements, the assistance of Dr. Andrew Solovyov and Dr. Namal DeSilva with solution ^{1}H NMR characterization, and the assistance of Dr. Sonjong Hwang at the Caltech Solid-State NMR facility are greatly appreciated. We also acknowledge ANPCYT (PICT 06-17492), Argentina; CONICET (PIP 6075), Argentina; CONICET-CNPq-NSF collaborative research agreement (CIAM program), and LNLS, Campinas, Brazil (project D04B-XAFS1-3492). V.I.K. acknowledges the technical assistance of Dr. A. Drapailo for the synthesis of the homooxacalix[3]arene **3a** and financial support from the Science & Technology Center in Ukraine Grant 3655. J.M.N. acknowledges the National Science Foundation for a graduate fellowship.

Supporting Information Available: Characterization of compound **4a**, alternate perspectives for the proposed structure of **3c** (Scheme S1), FTIR spectrum of **3a**, **1c**, **3c**, and **3c** after exposure to *tert*-butyl hydroperoxide (Figure S1), UV−visible spectra of **3a**, **3c**, and **4a** under different conditions (Figure S2), and TGA of **3a** and **3c** (Figure S3). This material is available free of charge via the Internet at http://pubs.acs.org.

JA065830C

(87) Imamura, S.; Nakai, T.; Kanai, H.; Shiono, T.; Utano, K. *Catal. Lett.* **1996**, *39*, 79−82.
(88) Yudanov, I. V.; Gisdakis, P.; Di, Valentin, C.; Rosch, N. *Eur. J. Inorg. Chem.* **1999**, *12*, 2135−2145.
(89) Sever, R. R.; Root, T. W. *J. Phys. Chem. B* **2003**, *107*, 4090−4099.